CHEMISTRY
AN ASIAN JOURNAL
www.chemasianj.org

Accepted Article

Title: Synthesis of N-doped Mesoporous Carbon Nanorods through Nano-confined Reaction: High Performance Catalyst Support for Hydrogenation of Phenol Derivatives

Authors: Xueteng Liu, Fei Pang, and Jianping Ge

To be cited as: *Chem. Asian J.* 10.1002/asia.201800112

Link to VoR: http://dx.doi.org/10.1002/asia.201800112

A Journal of

ACES
Asian Chemical Editorial Society

A sister journal of **Angewandte Chemie** and **Chemistry – A European Journal**

WILEY-VCH

10.1002/asia.201800112

WILEY-VCH

FULL PAPER

Synthesis of N-doped Mesoporous Carbon Nanorods through Nano-confined Reaction: High Performance Catalyst Support for Hydrogenation of Phenol Derivatives

Xueteng Liu, Fei Pang and Jianping Ge*[a]

Abstract: Traditional hard-template method for the preparation of mesoporous carbon structures has been well developed, but it may have difficulty in complete filling of organic precursors in ordered mesochannels and exact replication of the templates. Here, mesoporous carbon nanorods (meso-CNRs) are synthesized through thermal condensation of furfuryl alcohol followed by the nano-confined decomposition of polyfurfuryl alcohol in silica nanotubes (SiO_2 NTs) with porous shells. Limited and slow releasing of gaseous water through the porous shells and finite polyfurfuryl precursor inside silica nanotubes are responsible for the formation of mesoporous structures. Nitrogen can be doped to the meso-CNRs by adding guanidine hydrochloride to the precursors. The nitrogen dopant not only stabilize the ultrasmall and active Pd nanocatalyst in meso-CNRs but also increase the electron density of Pd and accelerate the dissociation of H_2, both of which increase the catalytic activity of Pd catalyst in hydrogenation reactions.

Introduction

The structural design, synthesis and application of porous carbon materials have received considerable attention in the past decades due to their extraordinary physicochemical properties, including high surface area[1], large pore volume[2], adjustable pore size[3], chemically inert nature[4], mechanical stability[5], good conductivity[6] and low cost of manufacture. These outstanding features make porous carbon ideal materials which are widely used for electrode in fuel cells[7], supercapacitors[8] and energy storage[9]. It can also be used as sorbents for gas storage[10] and supports for many important catalytic processes[11]. Among these applications, carbon materials have a long history serving as superior supporting materials in heterogeneous catalysis, particularly as supports of precious metals for organic reactions including hydrogenation, dehydrogenation, oxidation and reduction. Because they are usually very stable at different pH environment in the absence of oxygen, and they also have high surface area for loading of dispersed metal catalyst.

In the past decades, soft- and hard-template methods have been proven to be most successful ways for the preparation of porous carbon structures with well-defined pore structures and narrow pore-size distributions.[12] Soft-template method using amphiphilic molecules to fabricate porous carbon materials is based on the chemical interactions between carbon precursors and soft templates and thereby the supramolecular assembly.[13] For example, Zhao et al. have synthesized N-doped ordered mesoporous carbon with a high nitrogen content through an evaporation-induced self-assembly process, which used a low-molecular-weight soluble resol as carbon source and dicyandiamide as nitrogen source.[13d] In addition to the soft-template strategy, ordered microporous, mesoporous and macroporous carbon materials can also be obtained by utilizing zeolite, mesoporous silica or aluminum oxide etc. as hard templates[14], which have less requirements for carbon precursors compared to the soft-templating method. For example, MacLachlan et al. have preserved the chiral nematic structure in films of nanocrystalline cellulose by filling the cellulose network with tetraethyl orthosilicate followed by its hydrolysis process. The as-formed silica served as a hard template for the carbonization of the cellulose at 900 °C, so that chiral nematic carbon films could be obtained after removal of the silica by treatment with sodium hydroxide.[14d] Ding et al. have prepared mesoporous carbon supported nitrogen-doped carbon by pyrolysis of polyaniline coated on CMK-3. The obtained N-doped porous carbon is used as electrocatalyst, which exhibits excellent performance towards ORR in alkaline media.[14e] Although the hard-template route is a universal method for various materials including carbon, it may have difficulty in complete filling of organic precursors in ordered channels or mesopores of templates, so that the inversed mesoporous structures are difficult to be reserved exactly and the yield is sometimes unsatisfactory compared to the templates.[15]

In this work, we reported a “nano-confined reaction” to prepare mesoporous structures, in which the precursors were confined in a hollow reactor with porous shells and the gas releasing reaction inside the nanoreactor produced the disordered mesoporous structures. Following this idea, mesoporous carbon nanorods (meso-CNRs) were prepared through thermal polymerization of furfuryl alcohol (FA) and confined pyrolysis of polyfurfuryl alcohol (PFA) inside a tubular SiO_2 “nanoreactor” followed by the removal of silica shells. Finite furfuryl precursors inside silica nanotubes and limited releasing of gaseous water through the porous shells were responsible for the mesoporous structures. The relevant experiments and discussions were performed to verify the mechanism of nano-confined reaction, which exhibited great potentials to prepare various mesoporous materials for catalysis, energy storage and electrochemical processes. It is also worth noting that the nitrogen dopant could be flexibly introduced to the mesoporous carbon through the addition of guanidine hydrochloride into the furfuryl alcohol solution in synthesis. The as-prepared N-doped meso-CNRs (N-meso-CNRs) shall be proved as a better support than meso-CNRs for Pd nanocatalyst in hydrogenation of phenol derivatives.

[a] X. Liu, F. Pang, Prof. J. P. Ge
Shanghai Key Laboratory of Green Chemistry and Chemical Processes, School of Chemistry and Molecular Engineering, East China Normal University
Shanghai, 200062 (P.R. China)
E-mail: jpge@chem.ecnu.edu.cn

10.1002/asia.201800112

Results and Discussion

Mesoporous carbon nanorods (meso-CNRs) are prepared by the loading of furfuryl alcohol (FA) and oxalic acid catalyzed polymerization of furfuryl alcohol, followed by nano-confined pyrolysis of polyfurfuryl alcohol (PFA) in the nanotubes successively. According to previous research works[16], the SiO_2 NTs with hollow cavity and mesoporous shell are first synthesized by etching ordered mesoporous SiO_2 NRs with PEI, which serves as protective agent and etchant at the same time. Furfuryl alcohol is loaded via soaking the nanotubes in a concentrated solution of furfuryl alcohol (40 vol%) and oxalic acid, followed by separation with centrifugation. Then, furfuryl alcohol filled in the nanotubes is polymerized under the catalysis of oxalic acid at 100 °C to produce polyfurfuryl alcohol (PFA/SiO_2 NRs). The precursors are decomposed to carbon through calcination at 550 °C in several hours to produce the composite of carbon and SiO_2 (carbon/SiO_2 NRs). Finally, meso-CNRs are obtained by removing the silica shells using an HF solution. (Figure 1) SEM and TEM images show that the mesoporous SiO_2 NTs prepared by surface-protected etching have typical tubular structure with disordered mesopores in the shells. The meso-CNRs are mostly porous nanorods mixed with few irregular impurities, which might be produced by the FA residuals left outside the nanotubes during the precursor loading. Diameters of meso-CNRs are apparently smaller than that of SiO_2 NTs, which suggests that the nanorods might be produced inside the nanotubes. Apparently, this reaction does not follow the mechanism of traditional hard-templating, because no mesoporous carbon nanotubes is produced through exact replication.

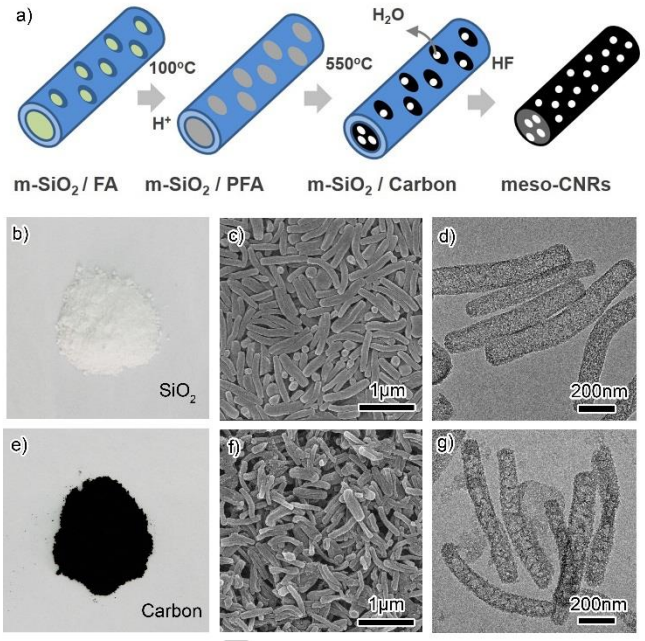

Figure 1. (a) Synthetic process and formation mechanism of meso-CNRs. Digital photos, SEM and TEM images of (b-d) SiO_2 NTs and (e-g) meso-CNRs.

Different from the traditional hard-templating strategy, the formation of meso-CNRs can be explained by a gas-releasing pyrolysis reaction confined in a nanosize "reactor". (Figure 2) In a hard-templating process, the products are usually exact replicas of the templates so that the products in above synthesis should have retained their tubular morphologies rather than rod-like structures. The absence of porous templates inside the hollow cavity of SiO_2 NTs cannot explain the large amount of mesopores in the meso-CNRs either, as shown in the cross-section TEM images. In addition, the surface area of the product from hard-templating is generally close to that of the template. However, the surface area of meso-CNRs (550 m^2/g) is actually higher than that of SiO_2 NTs (89 m^2/g). (Figure 2c and 2f) All these inconsistencies suggest that the current synthesis does not follow the traditional hard-templating mechanism. In fact, meso-CNRs are prepared by gas-releasing pyrolysis reaction confined in a nanosize "reactor". As a direct proof, the external diameters of meso-CNRs are approximately equal to the inner diameters of SiO_2 NTs. (Figure 2g and 2h) The thin porous shells of the SiO_2 NT function not as the template but as a permeable wall, which prevents the immediate release of the produced gaseous water, so that the retained tiny gas bubbles lead to the formation of a porous structure during pyrolysis. The limited furfuryl alcohol precursor inside the SiO_2 NTs is also favorable to the porous structure but not to the massive bulk structures in large dimensions, as the gaps and holes are inevitable due to untight packing of carbon structure. Both reasons are responsible for the formation of meso-CNRs, where such reaction can be summarized as a nano-confined gas-releasing reaction. In a parallel decomposition of polyfurfuryl alcohol without SiO_2 NTs, the precursors are continuously pyrolyzed to form massive bulk products because the produced water vapor quickly diffuses into the atmosphere, leaving behind a dense packing of carbon structures.

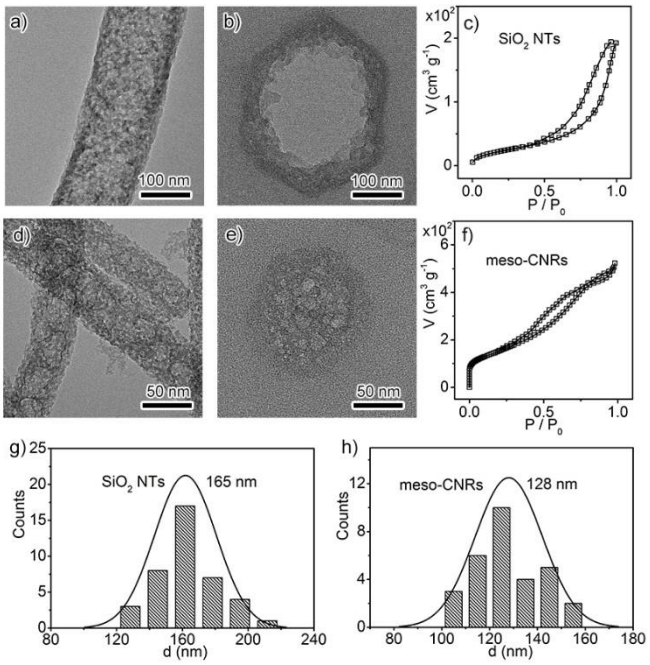

10.1002/asia.201800112

Figure 2. (a, d) Axial and (b, e) cross-sectional TEM images, (c, f) N_2 adsorption-desorption isotherms and (g, h) distribution of the external diameters of SiO_2 NTs and meso-CNRs.

According to the reaction mechanism, the prepolymerization of furfuryl alcohol into polyfurfuryl alcohol is a critical step for the production of meso-CNRs in the nano-confined reaction. It is known that furfuryl alcohol will condense to form polyfurfuryl alcohol in the presence of acidic catalysts at 100 °C.[17] (Scheme 1) The polymerization of furfuryl alcohol can be judged from the disappearance of IR peaks of O-H stretching at 3300 cm^{-1} and those in fingerprint region (1300-400 cm^{-1}). In order to verify the proposed reaction mechanism, we have made small changes to the loading and prepolymerization of furfuryl alcohol before thermal pyrolysis, which are expected to disclose the influence of "precursors" upon the products. Precursor A is SiO_2 NTs loaded with furfuryl alcohol only while Precursor B is SiO_2 NTs loaded with furfuryl alcohol and oxalic acid. Neither of them was prepolymerized before thermal pyrolysis. Precursor C and D correspond to the SiO_2 NTs loaded with the mixture of furfuryl alcohol and oxalic acid, which are prepolymerized at 100 °C for 30 and 120 min. The FTIR spectra show that Precursor A and B retain the absorption at 3300 cm^{-1} and the absorptions in fingerprint region, while those peaks nearly disappear for Precursor C and D. (Figure 3a) It indicates that both the acidic catalyst and thermal pretreatment are essential conditions for the polymerization of furfuryl alcohol. After calcination of the above four precursors at 550 °C, four kinds of composites (possibly C/SiO_2 NRs) are obtained, which are named as Intermediate Product A to D. They show 8%, 15%, 33% and 45% weight loss respectively from 100 °C to 800 °C. (Figure 3b) The higher weight loss of Intermediate Product C and D indicates that more carbon is produced during the calcination, compared to that of Intermediate Product A and B. TEM images also verify the formation of carbon for Product C and D. (Figure 3c-3f) It suggests that the effective loading of polyfurfuryl alcohol for Product C and D prevents evaporation of furfuryl alcohol. But for Product A and B, the evaporation of furfuryl alcohol results in the loss of carbon source during the temperature-rise process before calcination. These results are consistent with the FTIR spectra, which once again prove the necessity of prepolymerization to the production of meso-CNRs. In a word, meso-CNRs can be generated only when furfuryl alcohol loaded in the SiO_2 NTs is prepolymerized into polyfurfuryl alcohol before calcination. Otherwise, furfuryl alcohol will evaporate before calcination, so that there will be no carbon source to form mesoporous carbon structures.

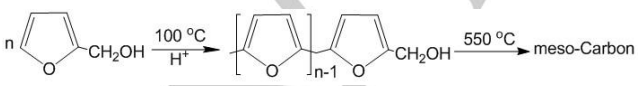

Scheme 1. Synthesis of meso-CNRs through polymerization of furfuryl alcohol and pyrolysis of polyfurfuryl alcohol.

Based on the synthesis of meso-CNRs, one can find that the keys to the nano-confined reactions are the synergetic combination of a confined "nano-reactor" and an appropriate gas-releasing reaction. As the name implies, the confined "nano-reactor" plays the role of a reaction container in nanoscale where the reaction is controlled well. Generally, the nano-reactor is chemically inert to avoid undesirable reaction with the reactants. A hollow interior cavity and porous shell are necessary so that there are enough precursors loaded into the reactor, and the reaction inside each reactor is equally controlled in kinetic aspects under the same macroscopic condition. The reactor should be easily removed to obtain the nanostructures of product. Obviously, the SiO_2 NTs obtained through "protective etching" could be an ideal "nano-reactor", because the nanotubes have a hollow interior cavity surrounded by porous shells which provide an ideal place for the pyrolysis of polyfurfuryl alcohol. In addition, silica has good thermal stability and is easily removed by HF. On the other hand, a mild gas-releasing process is also essential to fabricate the mesoporous structures. For meso-CNRs, the confined reaction works only when water vapor can be slowly released through the porous silica shell and the detained gas bubbles can contribute to the generation of mesoporous structures. Therefore, the synthesis won't be successful if the gaseous byproducts (H_2O) are generated asynchronously with the formation of main product (Meso-CNRs).

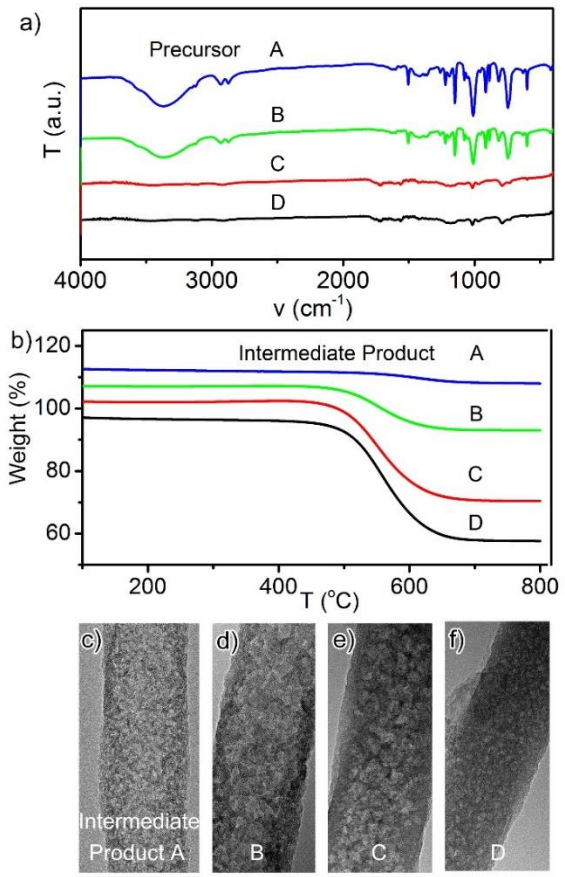

Figure 3. (a) FTIR spectra of 4 kinds of furfuryl alcohol loaded SiO_2 NTs, labeled as Precursor A to D. (b) TGA and (c-f) TEM images of the correspondingly produced C/SiO_2 composites, labeled as Intermediate Product A to D.

Due to the similar pyrolysis of guanidine hydrochloride as furfuryl alcohol, the N-doped meso-CNRs (N-meso-CNRs) are easily obtained through the addition of guanidine hydrochloride as nitrogen precursor in the furfuryl alcohol solution. Guanidine hydrochloride (CH_6N_3Cl) containing three amidogens in a molecule is usually used as precursor for nitrogen doping because it forms nitrides with many elements at high temperature. Owing to the high boiling point, guanidine hydrochloride loaded inside the SiO_2 NTs is not volatile during the temperature raising process and might be reserved until the decomposition. At the calcination temperature, guanidine hydrochloride is pyrolyzed accompanied with the elimination of ammonia, and the produced ammonia diffuses out slowly through the porous silica shells, which is similar to the pyrolysis of PFA. A series of N-meso-CNRs with the surface nitrogen contents of 1.5, 2.7 and 4.8 wt% are prepared by controlling the dosage of guanidine hydrochloride (0.5, 1 and 2 g) in furfuryl alcohol solution (20 mL). The amounts of surface nitrogen are determined by XPS, and the samples are named as $N_{1.5}$-meso-CNRs, $N_{2.7}$-meso-CNRs and $N_{4.8}$-meso-CNRs respectively. The gradual introduction of nitrogen dopant is also supported by the Raman spectra, where the ratio of D band at 1339 cm^{-1} to G band at 1595 cm^{-1} (I_D/I_G) is a sensitive indicator to the ratio of amorphous carbon toward graphitic carbon, and thereby an indicator for doping of nitrogen in our case. The Raman spectra suggest that I_D/I_G ratios of meso-CNRs, $N_{1.5}$-meso-CNRs, $N_{2.7}$-meso-CNRs and $N_{4.8}$-meso-CNRs are 0.51, 0.61, 0.74, and 0.82 respectively. (Figure 4) The higher I_D/I_G ratio indicates that a larger amount of graphitic carbon are destroyed and more nitrogen atoms are successfully embedded into the framework of graphitic carbon[18], which is consistent with the nitrogen contents measured by XPS.

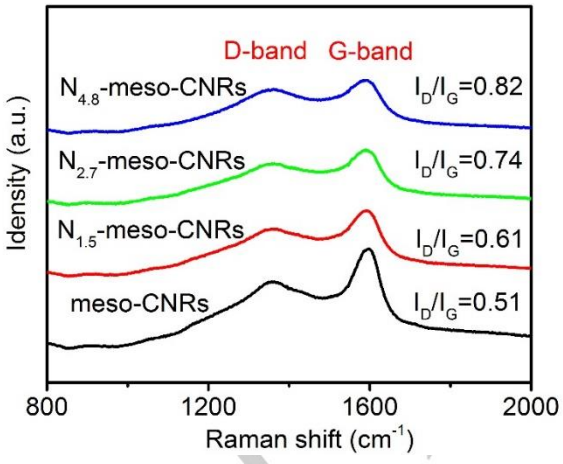

Figure 4. Raman spectra of meso-CNRs and N-doped meso-CNRs.

These N-meso-CNRs could be ideal supporting materials for the deposition of ultrasmall precious-metal nanoparticles. As a demonstration, Pd/N-meso-CNRs can be prepared by a deposition-precipitation (DP) method of palladium chloride followed by the reduction of palladium precursor. Its high-angle annular dark-field scanning TEM (HAADF-STEM) image shows that ultrasmall Pd nanoparticles are uniformly dispersed on the N-meso-CNRs. Energy dispersive spectrometer (EDS) mapping confirms that nitrogen is successfully introduced into the mesoporous carbon and Pd nanoparticles are uniformly dispersed on the obtained carbon materials. (Figure 5) The high surface area of N-meso-CNRs and the strong interactions between Pd nanoparticles and the nitrogen species will be favorable to the deposition of ultrasmall and highly dispersed Pd nanoparticles. At the same times, the high surface area and strong interactions would also contribute to the high activity for most heterogeneous catalysts.

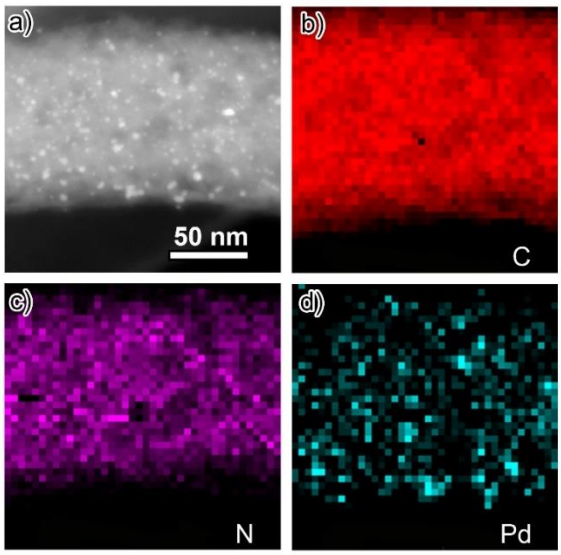

Figure 5. (a) HAADF-STEM images and (b-d) EDS mapping of Pd/N-meso-CNRs.

The as-prepared Pd/N-meso-CNRs are superior nanocatalysts for the hydrogenation of phenol derivatives due to the good dispersion of Pd nanoparticles on N-meso-CNRs. (Scheme 2) In a typical catalytic reaction, the aqueous solution of phenol derivatives (0.5 mmol) and Pd/$N_{4.8}$-meso-CNRs catalyst (53 mg) are loaded to a reaction tube, which is vacuumed and filled by H_2 with atmospheric pressure. After catalytic hydrogenation for several hours at specific temperature, the products are extracted from the reaction solution by toluene, which is analyzed by GC to determine the conversion of substrate and selectivity of target product. The catalytic results show that the conversion for phenol is 93.2% in 3 hours at 40 °C and the conversions for all phenol derivatives are above 85% in several hours at 80 °C, which is relatively higher than the previous work.[19] (Table 1) In addition, the selectivity is above 95% in all cases, which indicates that selective production of cyclohexanone could be achieved by the as-prepared Pd/N-meso-CNRs nanocatalysts. Although the Pd/$N_{4.8}$-meso-CNRs shows different activities for hydrogenation of phenol derivatives, their conversion and selectivity prove that it

10.1002/asia.201800112

is a universal catalyst for hydrogenation of a broad range of phenol substrate.

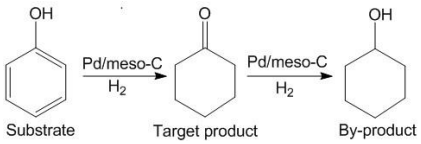

Scheme 2. Hydrogenation of phenol derivatives with Pd/N-meso-CNRs nanocatalyst.

Table 1. Hydrogenation of phenol derivatives by $Pd/N_{4.8}$-meso-CNRs nanocatalyst

Entry	Reactant	T (°C)	t (h)	Conv. (%)	Sel. (%)
1		40	3	93.2	97.3
2	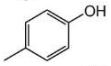	80	4	89.3	97.4
3	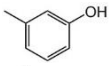	80	3	95	96.7
4		80	4	88.2	>99
5	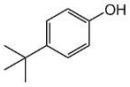	80	8	83.2	95.6
6	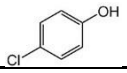	80	4	94.1	97.3

Reaction conditions: substrate (0.5 mmol), Pd (3.0 mol % relative to substrate), water (2.0 mL), H_2 (0.1 MPa).

The nitrogen content of N-meso-CNRs can be controlled by the guanidine hydrochloride in synthesis, which shows significant influence upon the activity of hydrogenation of phenol derivatives. EDS mapping and ICP-AES results reveal that Pd/meso-CNRs, $Pd/N_{1.5}$-meso-CNRs, $Pd/N_{2.7}$-meso-CNRs and $Pd/N_{4.8}$-meso-CNRs have similar Pd contents (2.87, 2.85, 2.83, and 2.92 wt%). However, when they are used in hydrogenation of phenol, the conversion reaches 52.2, 63.6, 78.6, and 93.2% respectively in 3 hours at 40 °C. (Table 2) The catalytic activities show a positive correlation with the nitrogen contents of these catalysts from 0% to 4.8%. Furthermore, this relationship can also be summarized from the kinetic curve of phenol hydrogenation. (Figure 6) Since the hydrogenation of phenol is a first-order reaction based on all the kinetic curves, its kinetic equation is summarized as $\ln(C_0/C_t) = kt$ and the slope is used to determine the rate constant.[20] C_0 and C_t are the concentrations of phenol before the reaction and at a specific reaction time. According to the kinetic curves, the rate constants of hydrogenation catalyzed by 4 Pd-catalysts are 0.254, 0.338, 0.485 and 0.731 h^{-1}. (Table 2) It suggests that a higher reaction rate can be achieved with a higher nitrogen content from 0% to 4.8% in the supporting materials of Pd-catalyst, which is consistent with the overall conversion in Table 2.

Table 2. Hydrogenation of phenol by 4 Pd catalysts

Cat.	N (wt%)	Conv. (%)	Sel. (%)	k (h^{-1})
Pd/meso-CNRs	0	52.2	98.8	0.254
$Pd/N_{1.5}$-meso-CNRs	1.5	63.6	98.4	0.338
$Pd/N_{2.7}$-meso-CNRs	2.7	78.6	98	0.485
$Pd/N_{4.8}$-meso-CNRs	4.8	93.2	97.3	0.732

Reaction conditions: phenol (0.5 mmol), Pd (3.0 mol % relative to phenol), water (2.0 mL), H2 (0.1 MPa), 40 °C, 3 h.

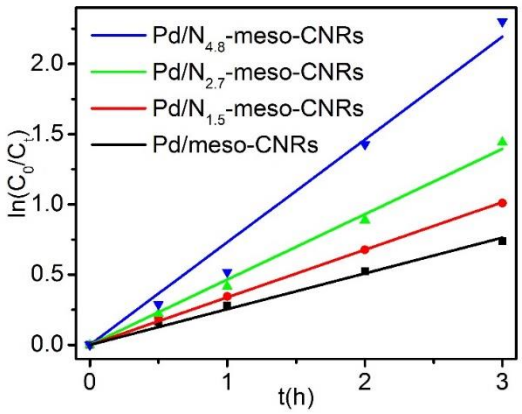

Figure 6. Kinetics curves of hydrogenation of phenol catalyzed by Pd/N-meso-CNRs.

The aforementioned dependence of catalytic activity upon the nitrogen contents of supporting materials can be explained by the stabilization of ultrasmall and highly active Pd nanoparticles by nitrogen species. It should be noted that the meso-CNRs and the other three N-meso-CNRs have almost the same structural characteristics except for the doping amount of nitrogen, and the Pd nanoparticles deposited on them are well dispersed without obvious agglomeration. (Figure 7) However, as the nitrogen content increases, the average diameter of Pd nanoparticles supported on meso-CNRs, $N_{1.5}$-meso-CNRs, $N_{2.7}$-meso-CNRs and $N_{4.8}$-meso-CNRs decreases in the sequence of 4.6, 3.6, 3.0 and 2.1 nm, respectively. It is known that the nitrogen dopant in the meso-CNR will coordinate to Pd atoms during the deposition, and the N-meso-CNRs with higher nitrogen contents will provide more coordination sites. In this case, Pd nanoparticles with smaller size tends to deposit on them since the overall Pd dosage are kept same. Therefore, the doping of nitrogen in meso-CNRs will contribute to the stabilization of ultrasmall and well-dispersed Pd nanocatalysts. Apparently, these smaller Pd nanoparticles will expose more active cites which effectively increase the activity of hydrogenation.

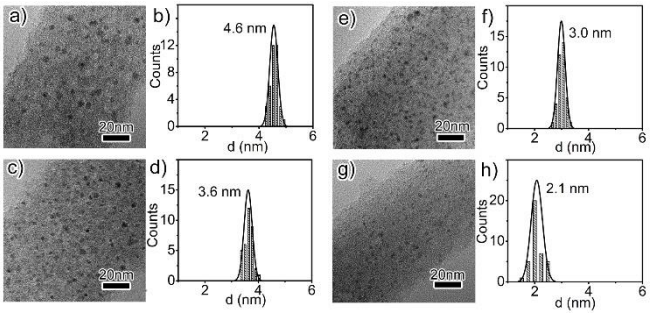

Figure 7. (a, c, e, g) TEM images of Pd/N-meso-CNRs with different N contents (0, 1.5, 2.7, 4.8 wt%) and (b, d, f, h) corresponding size distributions of deposited Pd nanoparticles.

The increasing of catalytic activity of Pd by doping of nitrogen in supports is also caused by the enrichment of electrons on Pd, and thereby an accelerated dissociation of H_2 to active H species in hydrogenation of phenol derivatives. In the XPS spectra of Pd-3d, the peaks at 335.8 eV and 341.1 eV are generally related to the metallic Pd^0 and those at 337.8 eV and 343.4 eV are related to Pd^{2+}.[21] The XPS spectra of four Pd-catalyst show that all the peaks shift 0.5 eV towards the lower binding energy, when the nitrogen contents gradually increase from 0 wt% to 4.8 wt%. (Figure 8) It is known that the decreasing of binding energy in XPS spectra is usually caused by the acquiring of extra electrons on corresponding atomic orbitals. For N-meso-CNRs, the lone pair electrons from nitrogen will coordinate to Pd, which increases the electron density of its internal 3d orbital and leads to the decreasing of binding energy.[21-22] For Pd nanoparticle loaded on the supports, N-meso-CNRs with higher surface nitrogen contents will coordinate to it at more positions, so that a higher electron density and a lower binding energy can be observed. Since the dissociation of H_2 into active H species on Pd catalyst is positively correlated to the electron density, the nitrogen dopant in supports will effectively increase the catalytic activity of Pd in hydrogenation of phenol derivatives.[21]

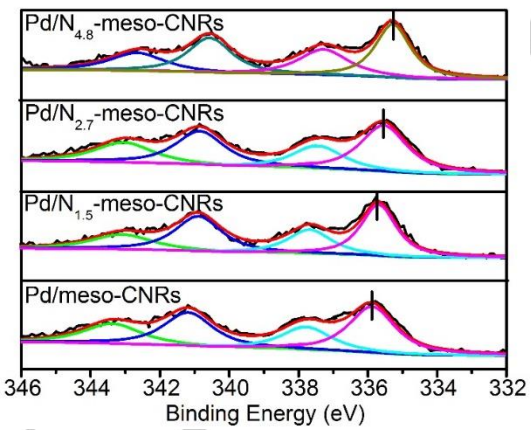

Figure 8. XPS spectra of Pd-3d for Pd/N-meso-CNRs with different nitrogen contents.

The as-prepared Pd/N-meso-CNRs show good stability in the hydrogenation of phenol. After 4 cycles of 3-hour reaction, the conversion of phenol decreases from 93.2% to 88% while the selectivity maintains above 97%. (Figure 9a) Here, the slight decrease of activity is probably because of the drop of Pd nanoparticles in liquid phase reaction, as the Pd content decreases from 2.92 wt% to 2.67 wt% according to ICP-AES measurement. TEM images of used catalysts reveal that they still have a good dispersion of Pd nanoparticles and no aggregation is induced during the reaction. (Figure 9b, 9c) The good stability of Pd catalyst can be attributed to the physical confinement from the mesoporous structures of carbon nanorods and the strong interactions between catalyst and support, which have been carefully discussed above.

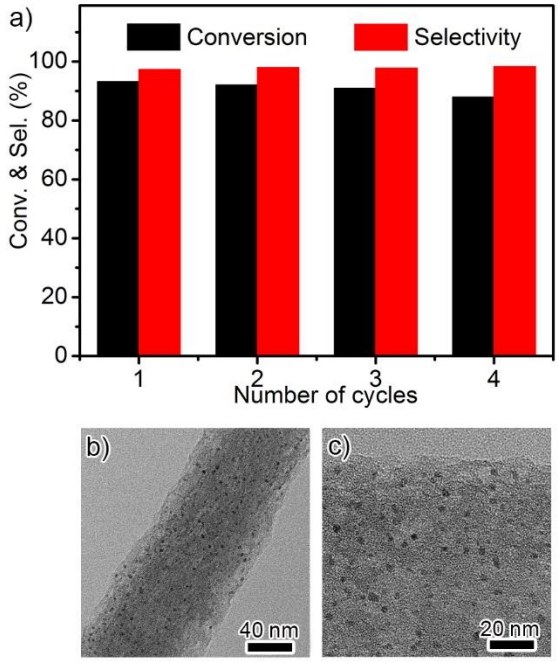

Figure 9. (a) Conversion and selectivity of 4 continuous phenol hydrogenation catalyzed by Pd/$N_{4.8}$-meso-CNRs. (b, c) TEM images of catalyst after 4 reactions.

Conclusions

In summary, mesoporous carbon nanorods are prepared through thermal condensation of furfuryl alcohol followed by the nano-confined decomposition of polyfurfuryl alcohol inside the SiO_2 nanotubes with porous shells. The formation of mesoporous structures is attributed to the controllable releasing of gaseous water and the limited precursor inside SiO_2 nanotubes, which is summarized as a nano-confined reaction mechanism. Due to the similar decomposition of guanidine hydrochloride compared to that of polyfurfuryl alcohol, the N-meso-CNRs with different nitrogen dopants are obtained by controlling the dosage of guanidine hydrochloride. With the increase of nitrogen contents, smaller Pd nanoparticles can be loaded on N-meso-CNRs due to

the interaction between Pd and N species, and a higher activity for hydrogenation of phenol can be realized. The nitrogen dopant can also enrich the electron density of Pd, accelerate the dissociation of H_2 and increase the catalytic activity. Furthermore, the as-prepared Pd/N-meso-CNRs show good stability and the highly dispersed Pd nanoparticles remain unchanged after catalytic reactions.

Experimental Section

Materials: Tetraethylorthosilicate (TEOS, 98%), hydrochloric acid (HCl, 37%), aqueous ammonia ($NH_3{\cdot}H_2O$, 28%), ethanol (99.7%), hydrofluoric acid (HF, 40%), palladium chloride ($PdCl_2$, 99%) and sodium borohydride ($NaBH_4$, 98%) were obtained from Sinopharm Chemical Reagent Co. Ltd. Furfuryl alcohol (98%), guanidine hydrochloride (98%) and phenol (99.9%) were purchased from Aladdin Co. Ltd. Triblock copolymer Pluronic F127, hexadecyltrimethylammonium bromide (CTAB, 96%), oxalic acid (98%) and aqueous solution of poly (ethyleneimine) (PEI, Mw=60000, 50 wt%) were purchased from Sigma-Aldrich. All the chemicals were directly used without further treatments.

Synthesis of SiO_2 nanotubes (NTs) by protective etching: SiO_2 NTs were prepared based on previous reference.[16] First of all, mesoporous SiO_2 NRs were synthesized by hydrolyzing TEOS in a basic solution at room temperature with CTAB and F127 as soft templates. Typically, F127 (1.23 g), CTAB (3 g) and $NH_3{\cdot}H_2O$ (28 wt%, 10 mL) were dissolved in water (300 mL) to form a colorless and transparent solution in an Erlenmeyer flask. TEOS (10 mL) was then injected to the above solution under stirring, which gradually transform to mesoporous SiO_2 nanorods within 2 hours. The nanorods were separated by centrifugation at 8000 rpm, washed three times with water and refluxed in the mixture of HCl (10 mL) and ethanol (200 mL) at 75 °C for 2 h to remove the surfactant molecules in the mesopores. Finally, all the emptied SiO_2 nanorods were dispersed in water as a stock solution with a concentration of 25 mg/mL. The stock solution (20 mL) was mixed with an aqueous solution of PEI (400 mL, 5 mg/mL), heated to 90 °C and maintained for 2 h to produce SiO_2 nanotubes. After cooling, the nanotubes were washed three times with water and dried in vacuum to obtain SiO_2 NTs powder (240 mg).

Synthesis of meso-CNRs and N-meso-CNRs through nano-confined reaction: The obtained SiO_2 NTs (240 mg) were mixed with the ethanol solution (20mL) of furfuryl alcohol (40 vol%) and oxalic acid (0.8 g) under stirring for 30 min to ensure the complete loading of precursors in SiO_2 NTs. Then, they were separated from the solution by centrifugation to obtain FA loaded SiO_2 NRs. The obtained FA/SiO_2 NRs were heated to 100 °C for 2 h so that furfuryl alcohol could be polymerized to form polyfurfuryl alcohol (PFA) under the catalysis of oxalic acid. The PFA/SiO_2 nanorods could be converted to meso-carbon/SiO_2 nanorods through calcination at 550 °C in N_2 for 4 h. Finally, pure meso-CNRs (160 mg) were obtained by removing silica with HF solution (20 mL, 10 wt%). The N-meso-CNRs were prepared through similar method except for the addition of a certain amount of guanidine hydrochloride into the furfuryl alcohol solution.

Preparation of Pd/N-meso-CNRs nanocatalyst and catalytic hydrogenation of phenol derivatives: The Pd/N-meso-CNRs (3 wt%) were fabricated by a modified deposition-precipitation method. In a typical process, an aqueous solution of H_2PdCl_4 (0.1 M) was first prepared by dissolving $PdCl_2$ (0.177 g) with HCl aqueous solution (10 mL, 10 vol%) at room temperature. At the same time, an aqueous suspension of N-meso-CNRs was prepared by mixing the nanorods (120 mg) with water (40 mL) under stirring for 1 h. After the addition of H_2PdCl_4 solution (0.34 mL, 0.1 M) into the above N-meso-CNRs solution, the pH value was regulated to 10.5 with NaOH solution (1 M) and Pd was deposited onto the N-meso-CNRs through addition of $NaBH_4$ aqueous solution (3.4 mL, 0.1 M). Finally, the Pd/N-meso-CNRs nanocatalyst (3 wt%) was obtained by centrifugation, washing with deionized water and drying in vacuum.

Catalytic tests were performed in a 50-mL reaction tube. In a typical process, the Pd/N-meso-CNRs nanocatalyst (53 mg), phenol derivatives (0.5 mmol) and water (2 mL) were first mixed in the reaction tube under stirring. Then, the reaction tube was vacuumed and purged with H_2 for three times, and it was attached to a balloon with H_2 to ensure the supply of H_2 during the hydrogenation. Subsequently, the reaction mixture was heated to a specific temperature and maintained for several hours. After the release of excessive H_2 and the cooling till room temperature, toluene was added to extract the product from the reaction solution, which was directly injected to the gas chromatography to analyze and calculate the conversion of phenol derivatives.

Characterization: Transmission electron microscope (TEM) images were captured by a FEI Tecnai G2 F30 microscope operated at 300 kV. The samples were embedded and cut using LEICA EM U27 for the observation of cross sections. Scanning electron microscope (SEM) images were captured by a Hitachi S-4800 microscope. Nitrogen adsorption-desorption isotherms and BET (Brunauer-Emmett-Teller) surface areas were measured by a Belsorp-Max analyzer at 77 K. X-ray photoelectron spectroscopy (XPS) measurements were performed on a Perkin-Elmer PHI 5000C ESCA system. Fourier transformed infrared (FTIR) spectra were recorded by Nexus 870 FTIR spectrometer. Raman spectroscopy measurements were carried out on a Thermo Scientific DXR. Thermogravimetric analysis (TGA) were carried out on a TGA/DSC 3+.Experimental Details.

Acknowledgements

This work is supported by the National Key Research and Development Program of China (2016YFB0701103), National Natural Science Foundation of China (21671067, 21471058) and ShuGuang Program supported by Shanghai Education Development Foundation and Shanghai Municipal Education Commission (15SG21).

Keywords: Nano-confined reaction • Mesoporous carbon • Catalyst support

[1] a) Z. J. Li, M. Jaroniec, Y. J. Lee, L. R. Radovic, *Chem. Commun.* **2002**, 1346-1347; b) Z. Ma, H. Zhang, Z. Yang, G. Ji, B. Yu, X. Liu, Z. Liu, *Green Chem.* **2016**, *18*, 1976-1982.

[2] a) X. Wang, Y. Li, *J. Mater. Chem. A* **2016**, *4*, 5247-5257; b) J. S. Yu, S. Kang, S. B. Yoon, G. Chai, *J. Am. Chem. Soc.* **2002**, *124*, 9382-9383; c) A. T. Rodriguez, M. Chen, Z. Chen, C. J. Brinker, H. Fan, *J. Am. Chem. Soc.* **2006**, *128*, 9276-9277; d) J. Wei, Z. Sun, W. Luo, Y. Li, A. A. Elzatahry, A. M. Al-Enizi, Y. Deng, D. Zhao, *J. Am. Chem. Soc.* **2017**, *139*, 1706-1713.

[3] a) Y. Meng, D. Gu, F. Q. Zhang, Y. F. Shi, H. F. Yang, Z. Li, C. Z. Yu, B. Tu, D. Y. Zhao, *Angew. Chem. Int. Ed.* **2005**, *44*, 7053-7059; b) R. Ryoo, S. H. Joo, S. Jun, *J. Phys. Chem. B* **1999**, *103*, 7743-7746; c) Z. Wang, Y. Zhu, W. Luo, Y. Ren, X. Cheng, P. Xu, X. Li, Y. Deng, D. Zhao, *Chem. of Mater.* **2016**, *28*, 7773-7780.

[4] Y. Zhang, A. Wang, T. Zhang, *Chem. Commun.* **2010**, *46*, 862-864.

[5] Z. J. Li, W. F. Yan, S. Dai, *Carbon* **2004**, *42*, 767-770.

[6] H. Xue, T. Wang, J. Zhao, H. Gong, J. Tang, H. Guo, X. Fan, J. He, *Carbon* **2016**, *104*, 10-19.

[7] a) G. S. Chai, S. B. Yoon, J. S. Yu, J. H. Choi, Y. E. Sung, *J. Phys. Chem. B* **2004**, *108*, 7074-7079; b) Q. Lv, K. Li, C. Liu, J. Ge, W. Xing, *Carbon* **2016**, *98*, 126-137.

[8] a) B. You, F. Kang, P. Yin, Q. Zhang, *Carbon* **2016**, *103*, 9-15; b) H. Jiang, P. S. Lee, C. Li, *Energy Environ. Sci.* **2013**, *6*, 41-53; c) Q. Shi, R. Zhang, Y. Lu, Y. Deng, A. A. Elzatahrya, D. Zhao, *Carbon* **2015**, *84*, 335-346.

[9] H. Nishihara, T. Kyotani, *Adv. Mater.* **2012**, *24*, 4473-4498.

[10] a) J. Tang, J. Liu, R. R. Salunkhe, T. Wang, Y. Yamauchi, *Chem. Commun.* **2016**, *52*, 505-508; b) J. Kong, S. I. S. Shahabadi, X. Lu, *Nanoscale* **2016**, *8*, 1770-1788.

[11] a) T. Sun, L. Xu, S. Li, W. Chai, Y. Huang, Y. Yan, J. Chen, *Appl. Catal. B Environ.* **2016**, *193*, 1-8; b) H. Ba, Y. Liu, T.-P. Lai, D.-V. Cuong, J. M. Nhut, N. Dinh Lam, O. Ersen, G. Tuci, G. Giambastiani, P.-H. Cuong, *ACS Catal.* **2016**, *6*, 1408-1419; c) V. L. Budarin, J. H. Clark, R. Luque, D. J. Macquarrie, *Chem. Commun.* **2007**, 634-636; d) B. Chen, S. Shang, L. Wang, Y. Zhang, S. Gao, *Chem. Commun.* **2016**, *52*, 481-484; e) G. A. Ferrero, K. Preuss, A. B. Fuertes, M. Sevilla, M. M. Titirici, *J. Mater. Chem. A* **2016**, *4*, 2581-2589; f) Q. Yue, J. Li, Y. Zhang, X. Cheng, X. Chen, P. Pan, J. Su, A. A. Elzatahry, A. Alghamdi, Y. Deng, D. Zhao, *J. Am. Chem. Soc.* **2017**, *139*, 15486-15493; g) M. Wang, X. Wang, Q. Yue, Y. Zhang, C. Wang, J. Chen, H. Cai, H. Lu, A. A. Elzatahry, D. Zhao, Y. Deng, *Chem. Mater.* **2014**, *26*, 3316-3321.

[12] a) C. Liang, Z. Li, S. Dai, *Angew. Chem. Int. Ed.* **2008**, *47*, 3696-3717; b) S. H. Joo, S. J. Choi, I. Oh, J. Kwak, Z. Liu, O. Terasaki, R. Ryoo, *Nature* **2001**, *412*, 169-172; c) C. D. Liang, S. Dai, *J. Am. Chem. Soc.* **2006**, *128*, 5316-5317.

[13] a) T.-Y. Ma, L. Liu, Z.-Y. Yuan, *Chem. Soc. Rev.* **2013**, *42*, 3977-4003; b) A. Berenguer, T. M. Sankaranarayanan, G. Gomez, I. Moreno, J. M. Coronado, P. Pizarro, D. P. Serrano, *Green Chem.* **2016**, *18*, 1938-1951; c) Y. Meng, D. Gu, F. Zhang, Y. Shi, L. Cheng, D. Feng, Z. Wu, Z. Chen, Y. Wan, A. Stein, D. Zhao, *Chem. Mater.* **2006**, *18*, 4447-4464; d) J. Wei, D. Zhou, Z. Sun, Y. Deng, Y. Xia, D. Zhao, *Adv. Funct. Mater.* **2013**, *23*, 2322-2328.

[14] a) Z. X. Ma, T. Kyotani, A. Tomita, *Chem. Commun.* **2000**, 2365-2366; b) M. Kruk, M. Jaroniec, T. W. Kim, R. Ryoo, *Chem. Mater.* **2003**, *15*, 2815-2823; c) J. Lee, S. Han, T. Hyeon, *J. Mater. Chem.* **2004**, *14*, 478-486; d) K. E. Shopsowitz, W. Y. Hamad, M. J. MacLachlan, *Angew. Chem. Int. Ed.* **2011**, *50*, 10991-10995; e) J. Xu, S. Lu, X. Chen, J. Wang, B. Zhang, X. Zhang, C. Xiao, S. Ding, *Nanotechnology* **2017**, *28*.

[15] a) S. Schrettl, B. Schulte, H. Frauenrath, *Nanoscale* **2016**, *8*, 18828-18848; b) J. Zhang, F. Guo, X. Wang, *Adv. Funct. Mater.* **2013**, *23*, 3008-3014.

[16] L. You, T. Wang, J. Ge, *Chem. Eur. J.* **2013**, *19*, 2142-2149.

[17] S. Bertarione, F. Bonino, F. Cesano, S. Jain, M. Zanetti, D. Scarano, A. Zecchina, *J. Phys. Chem. B* **2009**, *113*, 10571-10574.

[18] T. C. Mendes, C. Xiao, F. Zhou, H. Li, G. P. Knowles, M. Hilder, A. Somers, P. C. Howlett, D. R. MacFarlane, *ACS Appl. Mater. Interfaces* **2016**, *8*, 35243-35252.

[19] Z. Li, J. Liu, C. Xia, F. Li, *ACS Catal.* **2013**, *3*, 2440-2448.

[20] Y. Li, X. Xu, P. Zhang, Y. Gong, H. Li, Y. Wang, *RSC Adv.* **2013**, *3*, 10973-10982.

[21] Y. Wang, J. Yao, H. Li, D. Su, M. Antonietti, *J. Am. Chem. Soc.* **2011**, *133*, 2362-2365.

[22] Y. Sun, C. Du, G. Han, Y. Qu, L. Du, Y. Wang, G. Chen, Y. Gao, G. Yin, *Electrochim. Acta* **2016**, *212*, 313-321.

10.1002/asia.201800112

WILEY-VCH

Entry for the Table of Contents

FULL PAPER

N-doped mesoporous carbon nanorods are prepared through the nano-confined decomposition in silica nanotubes with porous shells, in which limited and slow releasing of gaseous water and finite precursor inside silica nanotubes are responsible for the formation of mesoporous structures.

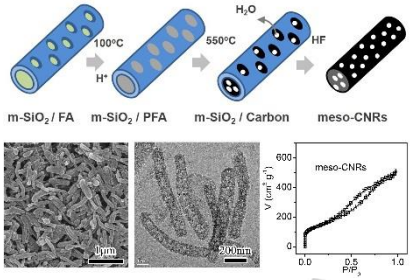

Xueteng Liu, Fei Pang and Jianping Ge[a]*

Page No. – Page No.

Synthesis of N-doped Mesoporous Carbon Nanorods through Nano-confined Reaction: High Performance Catalyst Support for Hydrogenation of Phenol Derivatives